Electronic Supplementary Material (ESI) for Lab on a Chip.
This journal is © The Royal Society of Chemistry 2018

Supplementary Materials

An Integrated Micro-Millifluidic Processing System

Authors
Jia Ming Zhang,[a†+] Qinglei Ji,[a†] Ying Liu,[a] Jianyong Huang[b] and Huiling Duan*[ac]

Affiliations

a. State Key Laboratory for Turbulence and Complex Systems, Department of Mechanics and Engineering Science, BIC-ESAT, College of Engineering, Peking University, Beijing 100871, People's Republic of China.

b. Department of Mechanics and Engineering Science, College of Engineering, Peking University, Beijing 100871, People's Republic of China.

c. CAPT, HEDPS and IFSA Collaborative Innovation Center of MoE, Peking University, Beijing, 100871, People's Republic of China.

†These authors contributed equally to this work.

+Present address: Physics of Fluids Group, University of Twente, The Netherlands
*hlduan@pku.edu.cn

This file includes:

1. Numerical results

TangoPlus (Stratasys Corp.) is a rubber-like photopolymer for the print of flexible parts. We measure its Young's module E = 0.504MPa within a deformation of up to 30%, and Poisson's ratio ν = 0.495-0.499 is provided by the provider. An elastic model in Abaqus (Dassault Systèmes) is used to study the deformation of flexible membranes. A finite volume model in ANSYS Fluent (ANSYS Inc.) is used for the estimation of flow fields. Fig. S1A shows the case of the check valve closure. The check valve with G=60 μm and α=90°used in our MPS is chosen to simulate. Under 100 mbar pressure the check valve is fully closed, which agrees well with our experimental results

in Fig. 3A. Fig. S1B shows the deformation of the pressure membrane under 60 mbar. 3.2mm×4mm×0.3mm membrane we use in our MPS is simulated here. The maximum displacement of the pressure membrane (450 μm) is larger than the local channel height 400 μm, which ensures to fully close the channel. 70 mbar is required to fully close the channel in the experiments, which agrees well with our numerical results. Fig. S1C depicts the deformation of the vacuum membrane under a vacuum -90 mbar. Such deformation can compensate the overflow introduced by the upstream pressure membrane. In the experiments, we find that the vacuum required for compensating the overflow is -100 mbar, which agrees well with our numerical results. Fig. S1D shows the flow field in a branch channel of the sorting unit without applied pressure on the membrane.

2. Compensation flow test via dual-membrane valve unit

The compensation flow is important for stable nanoliter droplet generation in MPS, so we made more test experiments to get the best value of applied vacuum for the compensation flow. We connect a glass capillary with ID 100 μm directly to the outlet of the dual-membrane valve unit. The change of the liquid meniscus in the capillary can reflect the stability of the output flow coming from the dual-membrane valve unit. As shown in the Fig. S2, when no vacuum is applied on the second membrane (Vacuum = 0 mbar), the liquid meniscus is moving far away from the reference origin. When the applied vacuum is small (Vacuum = -80 mbar), the liquid meniscus is more stable than the case of no vacuum applied, but still moves away from the reference origin. When the applied vacuum is larger (Vacuum = -120 mbar), the liquid meniscus recedes from the reference origin since the deformation of the second membrane is larger. When the applied vacuum reaches -100 mbar, the liquid meniscus almost stays at the reference origin, which shows the compensation works best under this vacuum value applied.

3. Microfluidic chip

Fig. S3A shows the commercial desktop 3D-printer (Titian-2). We remove the original z-direction build platform and resin tank from the printer and we place a customized chip bed above the light source (Fig. S3B). The chips are placed in the chip bed for the exposure. The chip bed can be adjusted in XY plane for the exposure alignment (Fig. S3C). The desired pattern is acquired by projecting an image on the resin (photopolymer) through a projector without a physical mask (image mask). The exposure resolution provided by this projector can reach 25 μm/pixel. As shown in Fig. S3D, we dip a drop of resin on the bottom substrate and gently cover a top substrate with pre-drilled holes. Then the resin fully spreads due to the surface tension. The white part in the image is exposed and cured and the black part is unexposed and uncured. With a superfast exposure (~1s), the resin is cured and

simultaneously bonded to the two substrates. Next, with a vacuum suction from the holes, the uncured resin can be removed and the microchannel is formed. The dimensions of typical microfluidic chips are shown in Fig. S3E. The height of the cured resin is 120 ± 5 μm.

As shown in Fig. S4A, shorter exposure time results in insufficient curing and some patterns are lost. Longer exposure time results in over-curing and desired patterns are smeared. 1.4 second exposure is optimum for our system. Fig. S4B shows that a minimum width of 25 μm can be built in a V-type structure, and a little sharpness of the pattern can be lost due to the capillary effects. Then we test the fabrication ability for microchannels. Fig. S4C shows the channels through our chip length. For 16 mm long, the minimum width available is 190 μm (Fig. S4C1). Due to the capillary effects, uncured resin is difficult to remove from a very small and long channel. However, the typical microfluidic function length is usually hundred micrometers. If the length of the channel is 640 μm and connected with wider ends, the capillary effects can be greatly reduced and ~ 50 μm channel can be precisely fabricated (Fig. S4C2). The typical nozzle size in the flow-focusing and T-junction structure we use is shown in Fig. S4D. Nanoliter droplets can be generated through these nozzles.

In addition, we explore another advantage of this method that substrates can be chosen with highly degree of freedom. Besides the rigid substrates (PMMA and glass) we use in the MPS, the soft substrate (PET) can also be used which is shown in Fig. S5A. This demonstrates a great potential for fabricating flexible instruments such as wearable devices. In order to achieve high exposure resolution, the printable region is usually small. For current 25 μm/pixel resolution, 24×24 mm^2 can be exposed, which may be infeasible in some applications which require large areas. Therefore, we develop an extended exposure method to increase the printable area. 24×48 mm^2 chip is fabricated (Fig. S5B). The movable chip bed can offer the possibility for twice exposure. We usually adopt a small overlap exposure area between two parts to make sure the resin is fully exposed to connect these two parts.

4. QR-code module.

The information stored in QR-code can be interpreted by a reading camera as input commands to automate our MPS. Fig. S6 shows a typical QR-code routine we develop for generation of pre-defined red and blue droplets in our MPS.

5. Chip holder

Chip-to-World interfaces is important for the development of microfluidics because it is not straightforward to input liquids from macro-world to the microchannel. It is not easy for conventional soft-lithography technique to

obtain a user-friendly and robust interface. A couple of studies on developing interfaces have been reported[53-55]. Here we develop a simple, robust and user-friendly interface (chip holder) for connecting our microfluidic chips to the motherboard, which only requires simple freehand operation. The chip holder is modularly designed and possesses highly customized ability for different chips. The characteristics of chip holder is listed in Table S1. Assembly of the chip holder is also demonstrated in supplementary Movie S4.

Fig. S7A shows a schematic of chip holder which is integrated with the motherboard. It includes a holder base, a chip base, two wrenches, the screws for the wrench connection and four O-rings. O-rings are located in the notch to ensure sealing. Rotating the wrench only by hands can easily open and close the chip holder for chips loading and unloading. Fig. S7B and 7C show the close and open state, respectively.

6. Supplementary Figures and Tables

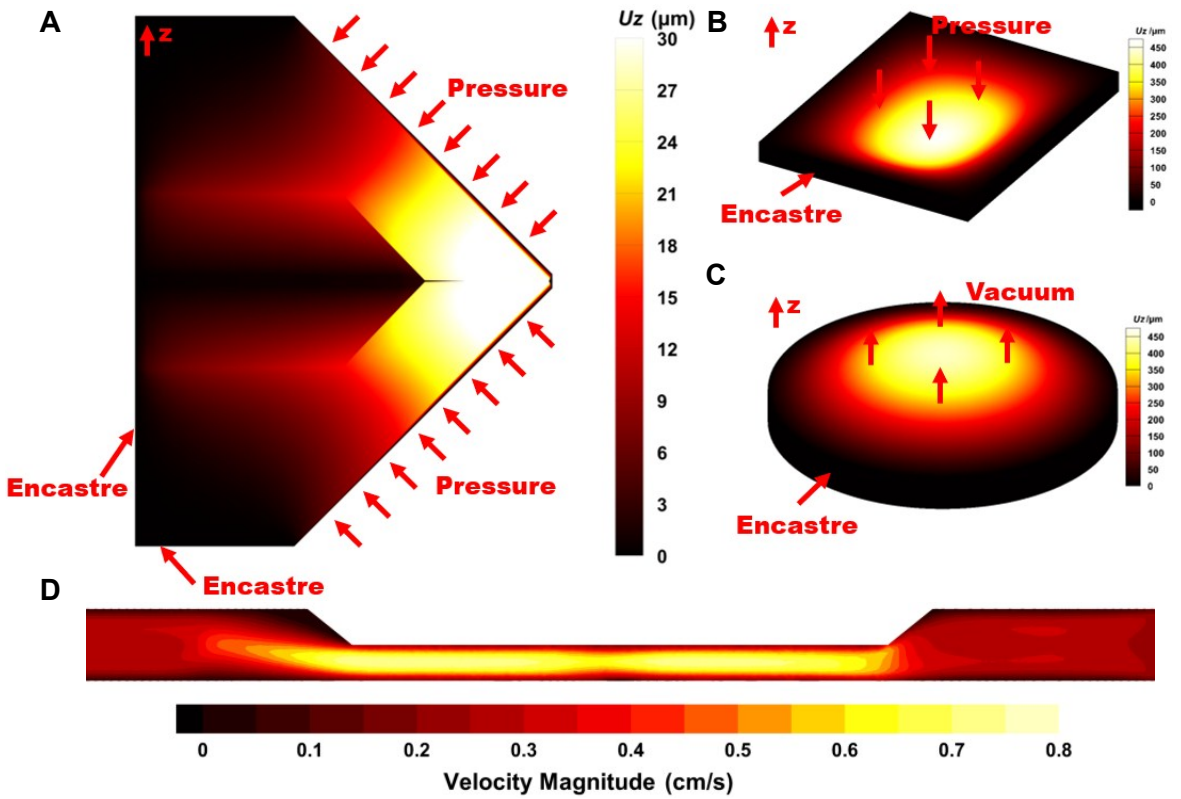

Figure S1 (**A**) Closed check valve. (**B**) Deformed pressure membrane. (**C**) Deformed vacuum membrane. (**D**) Velocity profile in the sorting channel without deformation.

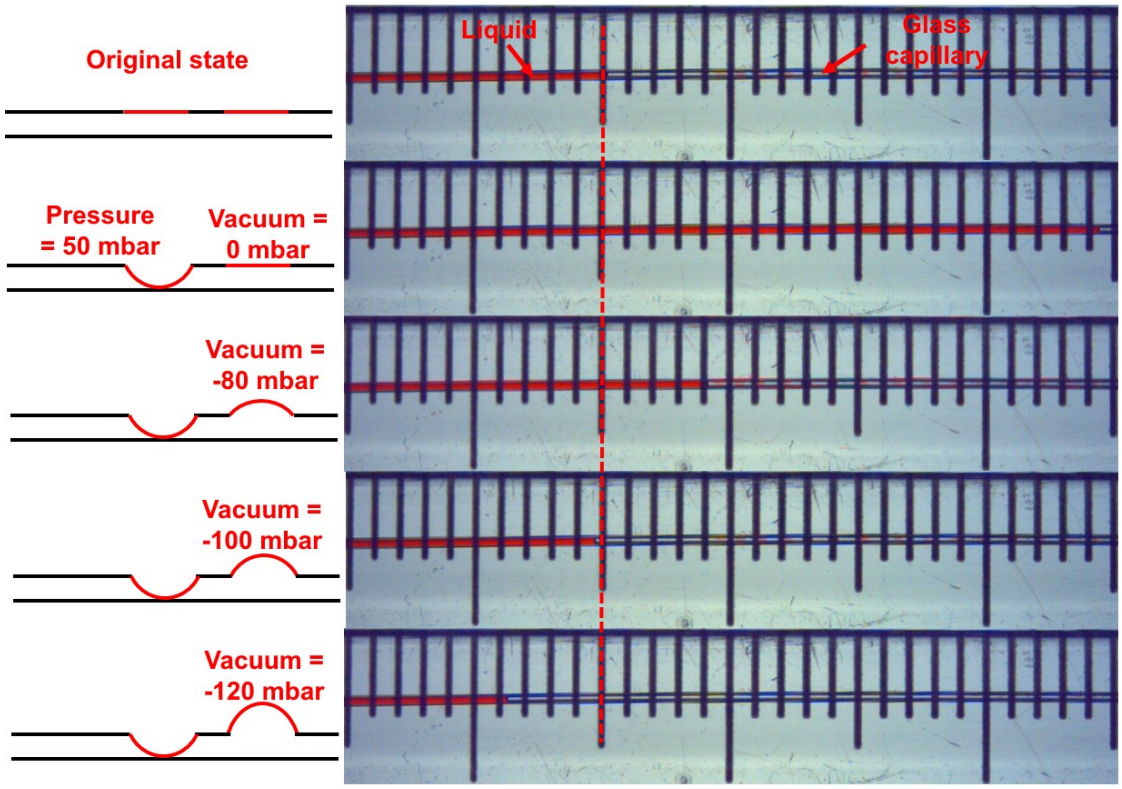

Figure S2 Experiments showing the compensation flow with different vacuum applied in dual-membrane valve unit.

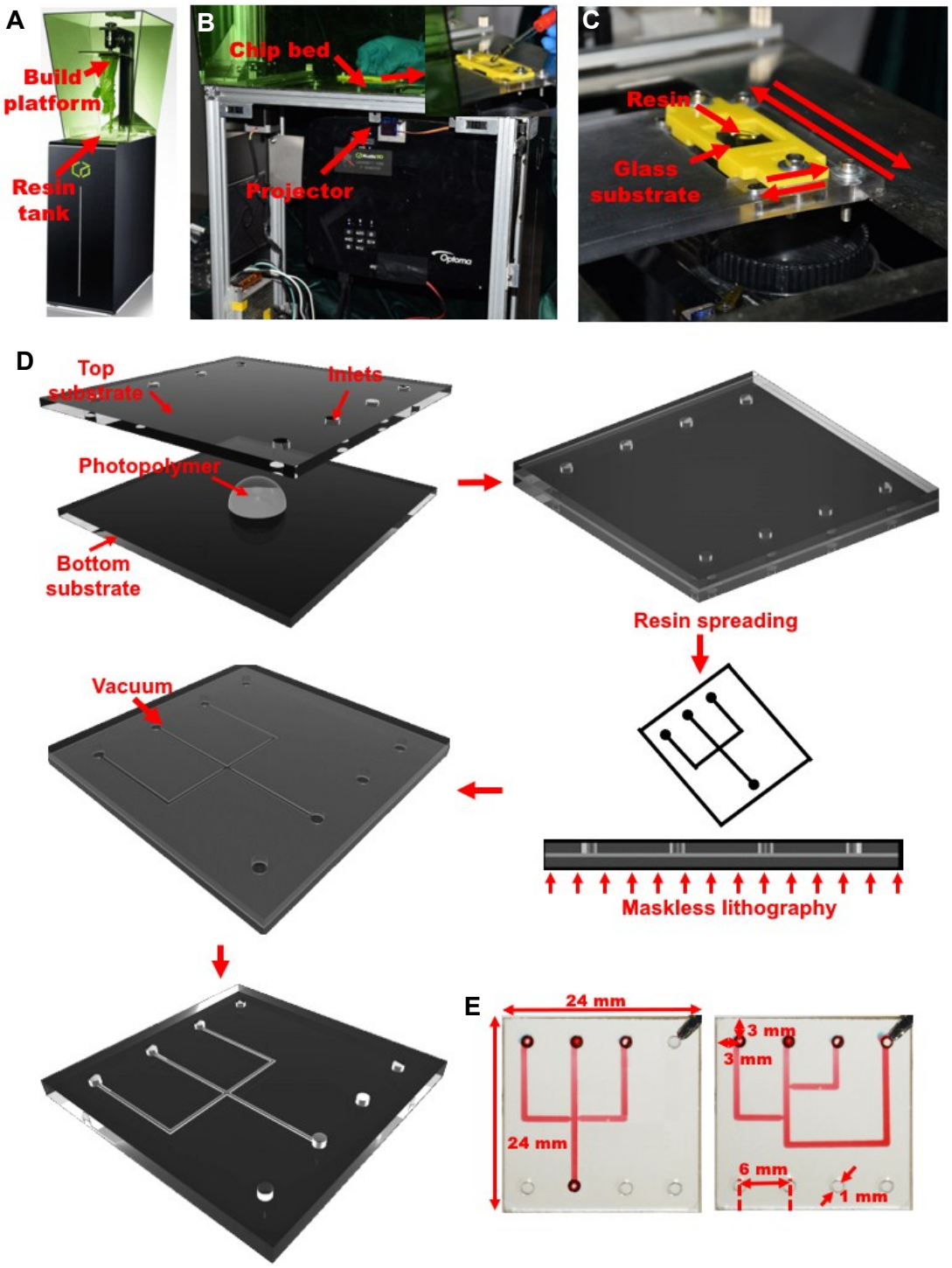

Figure S3 (**A**) Titian-2, 3D printer. (**B**) Our developed maskless lithography system. (**C**) The customized chip bed. (**D**) Fabrication process of a microfluidic chip. (**E**) Dimensions of the microfluidic chips.

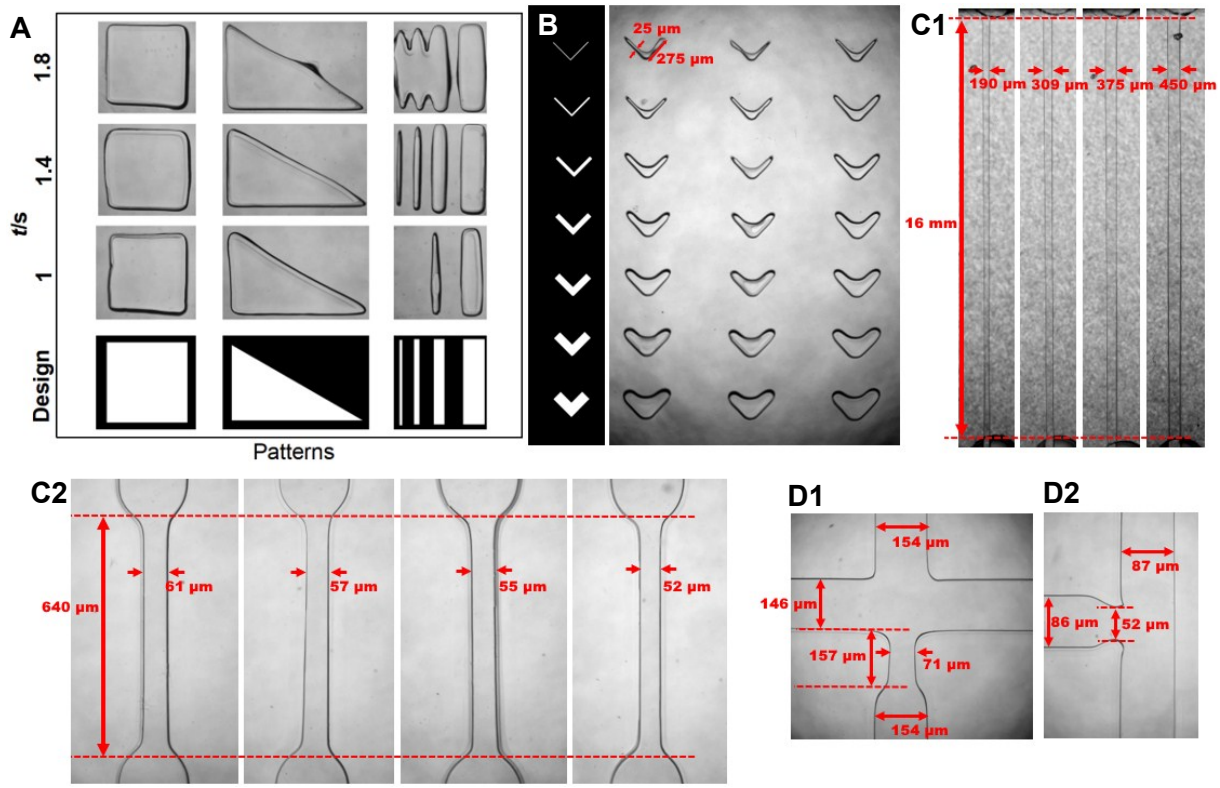

Figure S4 (**A**) Patterns acquired with different exposure time. (**B**) V-type structures. (**C**) Microchannel dimension test. (**D**) Dimensions of flow-focusing structure and T-junction structure for droplet generation.

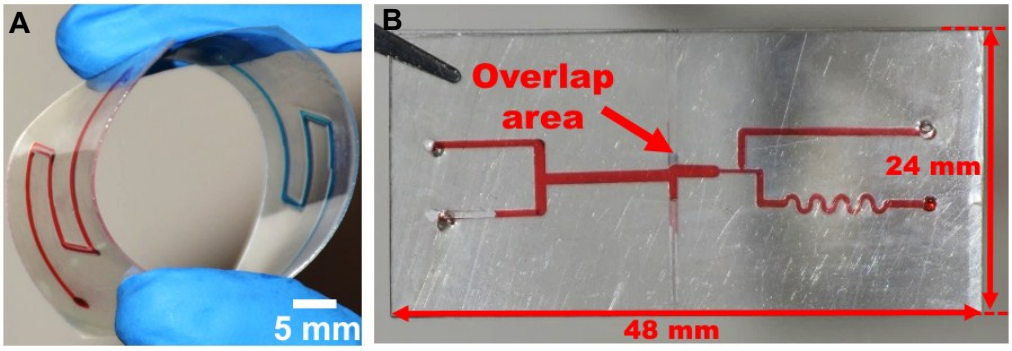

Figure S5 (A) Microfluidic chips with a flexible substrate (PET). (**B**) A microfluidic chip with extended area 24×48 mm^2.

Figure S6: The QR-code routine for droplet generation and manipulation.

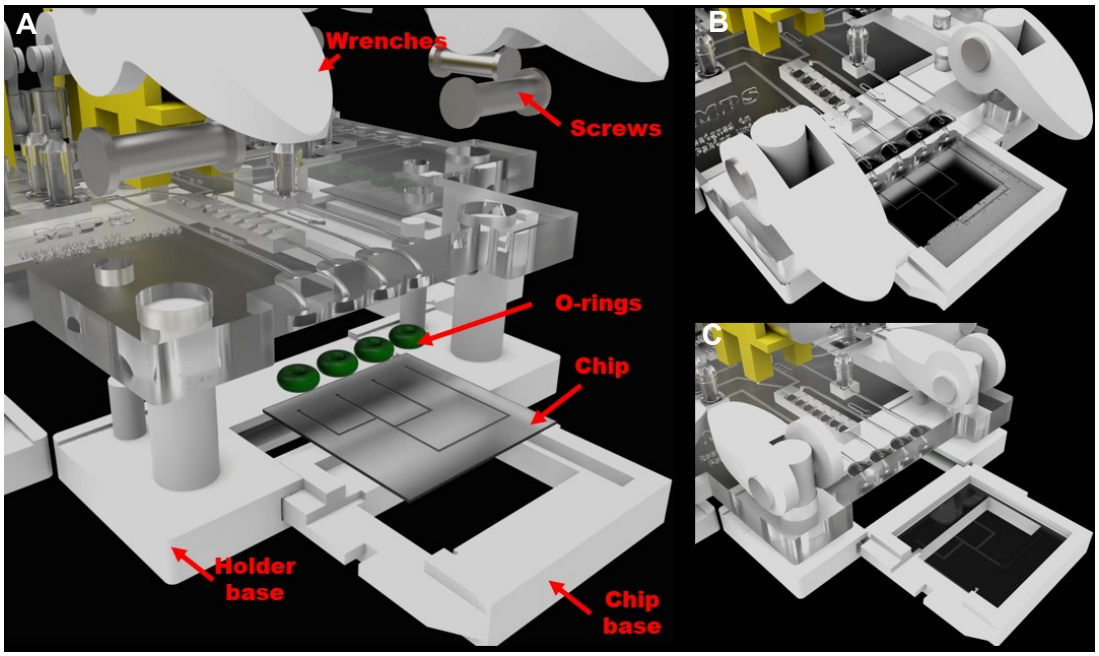

Figure S7: (**A**) Schematic of the chip holder. (**B**) Chip holder close state. (**C**) Chip holder open state.

Table S1: Characteristics of the chip holder.

Description	Parameter
Maximum operating pressure	0.4 MPa
Sealing material	Buna-N rubber/ fluorocarbon rubber (oil resistant)
O-ring ID	1mm (compatible 1/16” OD tubing)
Compatible chip thickness	0 ~ 6 mm
Compatible chip sizes	Customized

Table S2: Working state of the units at different stages with QR-code defined as *%R,5,M%B,5,L#R.*[a]

Progress	Red water pump	Blue water pump	Oil Pump	Red water valve	Blue water valve	Left branch channel	Middle branch channel	Right branch channel	QR-module	Remark
Prepare the system	○	○	○	○	○	○	○	○	○	*Initial state*
	○	○	—	○	○	○	○	○	○	*Fill channel with oil*
	—	—	—	○	○	○	○	○	○	*Adjust water position*
	○	○	—	○	○	○	○	○	—	*Read the QR message*
Generate red drops	—	○	—	○	—	—	○	—	○	*Pump the red water*
	○	○	—	—	—	—	○	—	○	*5 red drops generated*
Generate blue drops	○	—	—	—	○	○	—	—	○	*Pump the blue water*
	○	○	—	—	—	○	—	—	○	*5 blue drops generated*
Mission accomplished	○	○	○	○	○	—	—	—	○	*Pick the chip*
	○	○	○	○	○	○	○	○	○	*Turn off the MPS*

[a]**○: Close state —: Running state**

7. Legends of Supplementary Movies S1 to S5

7.1 Supplementary Movie S1:

On-chip pump for droplet generation.

This movie contains three video clips to demonstrate nanoliter droplet generation in USB-like microfluidic chips using our on-chip flow pumps. Food dyes are used in aqueous phase for enhancing visualization. The first video shows the droplet generation in flow-focusing structure with two on-chip pumps for the oil phase input and one on-chip pump for the aqueous phase input. All pump motors run at full speed of 1000 rounds per minute (rpm). The video is recorded with 3000 frames per second (fps) and played with 300 fps. The second video shows the droplet generation in double T-junction structure with two on-chip pumps for the aqueous phase input and one on-chip pump for the oil phase input. All pump motors run at full speed of 1000 rpm. The video is recorded with 1000 fps and played with 100 fps. The third video shows the droplet generation with programmable compositions. The pump for the blue aqueous phase input initially runs at 100 rpm to offer a relatively large flow rate. The pump for the red aqueous phase input initially runs at 1000 rpm to provide a relatively small flow rate. The rotating speeds for these two pumps vary reversely in 10 seconds. The video is recorded with 300 fps and played with 300 fps.

7.2 Supplementary Movie S2:

Droplet control with a single valve and a dual-membrane valve.

This video first shows the impact of overflow on the unexpected droplet generation when a single pneumatic valve is used for the fluid switching. When the dual-membrane valve is applied, the droplet generation can be ceased immediately and regenerate without unexpected droplets, which ensures the accurate number of droplet generation. The video is recorded with 60 fps and played with 30 fps.

7.3 Supplementary Movie S3:

Satellite droplet sorting.

This video demonstrates that satellite droplets are sorted to the side channel with different pressure applied on the branch channels. The video is recorded with 100 fps and played with 30 fps.

7.4 Supplementary Movie S4:

Assembly of the chip holder.

This video demonstrates how the chip holder works for loading USB-chips into the MPS, and is played at 25 fps.

7.5 Supplementary Movie S5:

Pre-defined number of droplet generation and distribution.

This video demonstrates that with a pre-defined QR-code *%R,5,M%B,5,L#R*, 5 red and 5 blue droplets are automatically generated and sorted into the designated channel. The video is recorded with 60 fps and played with 30 fps.